The American Journal of Chinese Medicine, Vol. 46, No. 3, 1–21

Institute for Advanced Research in Asian Science and Medicine
DOI: 10.1142/S0192415X18500349

Asatone Prevents Acute Lung Injury by Reducing Expressions of NF-κB, MAPK and Inflammatory Cytokines

Heng-Yuan Chang,[*] Yi-Chuan Chen,[*] Jaung-Geng Lin,[†] I-Hsin Lin,[*] Hui-Fen Huang,[*,§]
Chia-Chou Yeh,[*,¶] Jian-Jung Chen[*,//] and Guan-Jhong Huang[‡]

[*]*School of Post-Baccalaureate Chinese Medicine*
Tzu Chi University, Hualien 970, Taiwan

[†]*School of Chinese Medicine, College of Chinese Medicine*

[‡]*School of Chinese Pharmaceutical Sciences and Chinese Medicine Resources*
College of Chinese Medicine
China Medical University, Taichung 404, Taiwan

[§]*Department of Chinese Medicine, Taipei Tzu Chi Hospital*
Buddhist Tzu Chi Medical Foundation, Taipei 231, Taiwan

[¶]*Department of Chinese Medicine, Dalin Tzu Chi Hospital*
Buddhist Tzu Chi Medical Foundation, Chia-Yi 622, Taiwan

[//]*Department of Chinese Medicine, Taichung Tzu Chi Hospital*
Buddhist Tzu Chi Medical Foundation, Taichung 427, Taiwan

Published 29 March 2018

Abstract: Asatone is an active component extracted from the Chinese herb Radix *et* Rhizoma Asari. Our preliminary studies have indicated that asatone has an anti-inflammatory effect on RAW 264.7 culture cells challenged with lipopolysaccharide (LPS). Acute lung injury (ALI) has high morbidity and mortality rates due to the onset of serious lung inflammation and edema. Whether asatone prevents ALI LPS-induced requires further investigation. *In vitro* studies revealed that asatone at concentrations of 2.5–20 μg/mL drastically prevented cytotoxicity and concentration-dependently reduced NO production in the LPS-challenged macrophages. In an *in vivo* study, the intratracheal administration of LPS increased the lung wet/dry ratio, myeloperoxidase activity, total cell counts, white blood cell counts, NO, iNOS, COX, TNF-α, IL-1β, and IL-6 in the bronchoalveolar lavage fluid as well as mitogen-activated protein kinases in the lung tissues. Pretreatment with asatone could reverse all of these effects. Asatone markedly reduced the levels of TNF-α and IL-6 in the lung and liver,

Correspondence to: Dr. Guan-Jhong Huang, School of Chinese Pharmaceutical Sciences and Chinese Medicine Resources, College of Chinese Medicine, China Medical University, No. 91, Hsueh-Shih Road, Taichung 40402, Taiwan. Tel: (+886) 4-2205-3366 (ext. 5508), Fax: (+886) 4-2208-3362, E-mail: gjhuang@mail.cmu.edu.tw

but not in the kidney of mice. By contrast, LPS reduced anti-oxidative enzymes and inhibited NF-κB activations, whereas asatone increased anti-oxidative enzymes in the bronchoalveolar lavage fluid and NF-κB activations in the lung tissues. Conclusively, asatone can prevent ALI through various anti-inflammatory modalities, including the major anti-inflammatory pathways of NF-κB and mitogen-activated protein kinases. These findings suggest that asatone can be applied in the treatment of ALI.

Keywords: Acute Lung Injury; Asatone; Lipopolysaccharide; Antioxidative Enzymes; NF-κB; Mitogen-Activated Protein Kinases; Sepsis.

Introduction

Acute respiratory distress syndrome (ARDS), the most devastating form of acute lung injury (ALI), is a serious clinical disorder with a high mortality rate (30–60%) (Su *et al.*, 2012). ALI and ARDS are defined by a series of histologic changes, such as pulmonary edema and neutrophil accumulation, which are characterized by diffuse injury to the alveolar capillary membrane in the lung and associated with shock, sepsis, acidosis, and ischemia reperfusion (Tunceroglu *et al.*, 2013; Huang *et al.*, 2014a). However, no specific pharmacologic treatments for ALI/ARDS are available. Hence, the identification of new drugs that can reduce ALI/ARDS-associated inflammation is a major goal of pharmaceutical companies.

Lipopolysaccharide (LPS) is widely used for the induction of ALI/ARDS animal models; its similarity to human ALI renders it suitable for investigating pathogenesis and the therapeutic effects of potential drugs (Huang *et al.*, 2008; Chen *et al.*, 2010; Tsai *et al.*, 2014). LPS administration elicits a series of damaging effects on endothelial and epithelial cell integrity, lung edema, mass release of inflammatory mediators and chemotactic factors, and extensive neutrophil infiltration (Huang *et al.*, 2014a; Chien *et al.*, 2015). LPS induces inducible nitric oxide synthase (iNOS) and cyclooxygenase-2 (COX-2) over expression and nitric oxide (NO), tumor necrosis factor α (TNF-α), interleukin-1β (IL-1β), and interleukin-6 (IL-6) overproduction (Zamora *et al.*, 2000; Giuliano and Warner, 2002). Additionally, LPS elicits overproductions of superoxide anions ($O_2\bullet^-$) and their metabolites, such as hydrogen peroxide (H_2O_2), hydroxyl radicals, and hypochlorous acid (HClO) (Bhaskaran *et al.*, 2013; Li *et al.*, 2015a), causing increased permeability and damage to the alveolar capillary barrier. The activation of the inhibitor of kappa B (IκB), nuclear factor-κB (NF-κB), and mitogen-activated protein kinases (MAPKs) is a crucial step in the development of ALI/ARDS (Bhaskaran *et al.*, 2010; Liu *et al.*, 2011; Khan *et al.*, 2013; Huang *et al.*, 2014a). Thus, the identification of drugs that can target these ALI/ARDS-associated inflammatory mediators or important pathways to eliminate the inflammatory processes is of vital clinical concern.

Asatone (Fig. 1A) is a pharmacologically active component in the traditional Chinese herb Radix *et* Rhizoma Asari (*xixin*) (Hayashi *et al.*, 1976; Yamamura *et al.*, 1976). As one of the most important traditional Chinese medicines, *xixin* is used to treat the common cold,

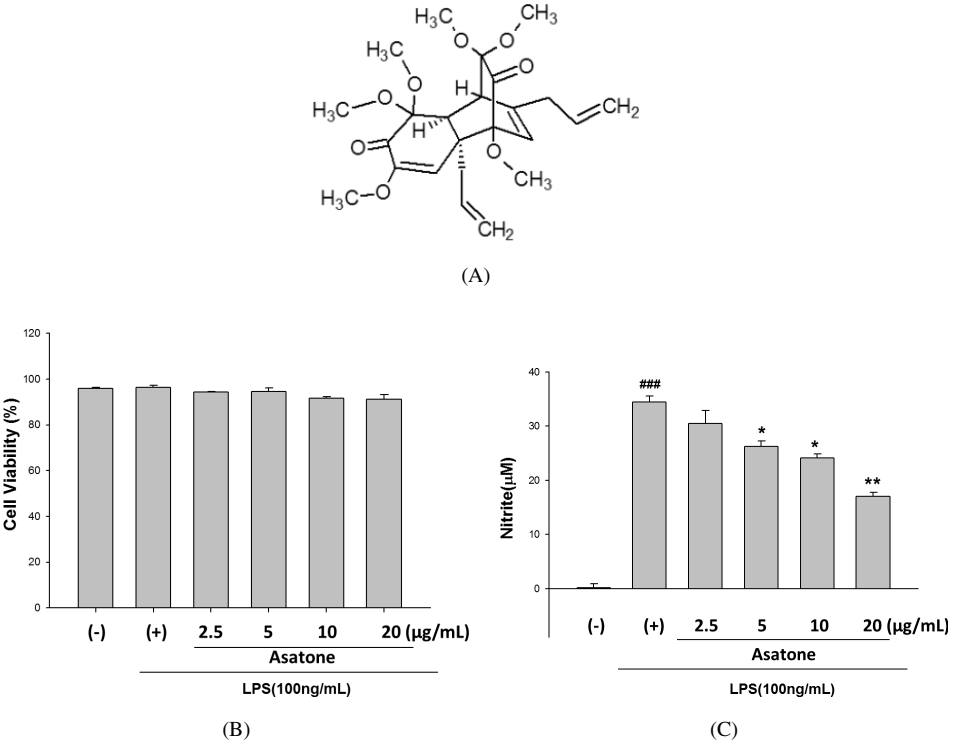

Figure 1. Asatone inhibited cytotoxicity and NO production in RAW 264.7 cells challenged by lipopolysaccharide (LPS). One hour prior to the addition of 100 ng/mL of LPS, the RAW cells were pretreated with different concentrations of asatone (0, 2.5, 5, 10, or 20 μg/mL) and cultured for 24 h. (A) The structure of asatone; (B) Cell viability was determined by ELISA; (C) NO production was quantified by ELISA. (−), saline alone; (+), LPS + saline. The data are presented as mean ± SD for the three different experiments performed in triplicate. $^{###}p < 0.001$ compared with the control group (one-way ANOVA followed by Scheffe's multiple range tests). $^{*}p < 0.05$ and $^{**}p < 0.01$ compared with the LPS group.

cough, sinusitis, headache, toothache, and rheumatic arthralgia (Drew *et al.*, 2002; Kim *et al.*, 2003; Wang *et al.*, 2015), according to the Chinese Pharmacopoeia. Moreover, due to its extensive biological activities, *xixin* has anti-inflammatory, antipyretic, antimicrobial, and analgesic properties (Kosuge *et al.*, 1978; Lee *et al.*, 2005; Dan *et al.*, 2010). However, the anti-inflammatory mechanism and the necessary therapeutic dose of asatone are rarely studied.

Our preliminary studies demonstrated that asatone appeared to have an anti-inflammatory effect on RAW 264.7 culture cells challenged with LPS. These effects were also observed *in vivo* in mice lungs that were subjected to LPS injuries. Asatone was further revealed to prevent ALI through various anti-inflammatory effects involving the major inflammatory pathways of IκB, NF-κB and MAPK. The present findings indicate that asatone may be an effective therapy for ALI by targeting these pathways.

Materials and Methods

Chemicals

Asatone (Fig. 1A) was purchased from BJYM Pharmaceutical and Chemical Co. Ltd. (Beijing, China), and LPS (*Escherichia coli* 055: B5), dexamethasone (DEX), 3-[4,5-dimethylthiazol-2-yl]-2,5-diphenyltetrazolium bromide (MTT), and other chemicals were purchased from Sigma Chemical Co. (St. Louis, MO, USA). TNF-α, IL-1β, and IL-6 were purchased from Biosource International Inc. (Camarillo, CA, USA). The primary antibodies against iNOS, COX-2, NF-κB, IκBα, ERK, JNK, p38, p-ERK, p-JNK, p-p38 and β-actin antibodies (Santa Cruz, CA, USA), and protein assay kits (Bio-Rad Laboratories Ltd., Watford, Hertfordshire, UK) were obtained as indicated. Polyvinylidene fluoride membrane (PVDF) was obtained from Millipore Corporation (Millipore Co., Bedford, MA, USA).

Cell Culture

A murine macrophage cell line RAW264.7 (BCRC No. 60001) was purchased from the Bioresources Collection and Research Center (BCRC) of the Food Industry Research and Development Institute (Hsinchu, Taiwan). Cells were cultured in plastic dishes containing Dulbecco's Modified Eagle's Medium (DMEM, Sigma, St. Louis, MO, USA) supplemented with 10% fetal bovine serum (FBS, Sigma, USA) in a CO_2 incubator (5% CO_2 in air) at 37°C and subculture every other day at a dilution of 1:5 using 0.05% trypsin 0.02% EDTA in Ca^{2+}, Mg^{2+} free phosphate-buffered saline (DPBS).

Cytotoxicity and NO Production

This experiment consisted of two parts. In the first part, we examined the viability of RAW cells, and in the second part, we examined NO production in the cell medium.

RAW 264.7 cells (2×10^4 per well) (Li *et al.*, 2015a) were seeded in 96-well plates containing DMEM supplemented with 10% FBS for 1 day to become nearly confluent. On the second day, the cells were pretreated with 2.5–20 μg/mL of asatone 1 h before treatment with LPS (100 ng/mL) at 37°C for 24 h. The medium was removed and stored for the NO experiments, and the cells were incubated with 100 μL of 0.5 mg/mL MTT in a CO_2 incubator (5% CO_2 in air) for 6 h at 37°C. The medium was discarded, followed by the addition of 100 μL of isopropanol. After incubation for 30 min, the absorbance was measured using a microplate reader at 570 nm. These steps were repeated three times for each concentration.

The nitrite level in cultured media, which reflects intracellular NO synthase activity, was determined using a Griess reaction (Hu *et al.*, 2014). One hundred microliters of Griess reagent (1% sulfanilamide, 0.1% naphthyl ethylenediamine dihydrochloride, and 5% phosphoric acid) was added to each sample medium and incubated at room temperature for 10 min. By using sodium nitrite to generate a standard curve, the concentration of nitrite for each sample was measured at 540-nm absorbance.

Animals

Seventy-two male mice aged 6 weeks were obtained from the Institute for Cancer Research, BioLASCO Co., Ltd., Taipei, Taiwan. The animals were kept in plexiglass cages at a constant temperature of $22 \pm 1\,^{\circ}C$, with a relative humidity of $55\% \pm 5\%$ and 12-h dark–light cycles. They were provided with food and water *ad libitum*. Animal studies were conducted according to the regulations of Institutional Animal Ethics Committee, and the protocol was approved by the Committee for the Purpose of Control and Supervision of Experiments on Animals.

Model of LPS-Induced ALI

The 72 male mice were randomly divided into six groups (each $n = 12$): a control group (distilled water *ad libitum*), an LPS (5 mg/kg) group, a DEX group (10 mg/kg), a low-dosage asatone group (LPS 5 mg/kg + asatone 10 mg/kg), a moderate-dosage asatone group (LPS 5 mg/kg + asatone 20 mg/kg), and a high-dosage asatone group (LPS 5 mg/kg + asatone 40 mg/kg). Half of each group were used for the inflammation protein analysis, slicing, and edema, and the rest were used for the bronchoalveolar lavage fluid (BALF) analysis.

ALI was induced by LPS (*E. coli* LPS serotype 055:B5, Sigma) through intratracheal injection (Zhang *et al.*, 2010). In brief, the mice were anesthetized with a mixed reagent of 10 μL/g through intraperitoneal injection (IP), urethane (0.6 g/mL) and chloral hydrate (0.4 g/mL), followed by DEX (10 mg/kg) or asatone through IP in individual doses. One hour later, 5 mg/kg LPS was administered in 50-μL sterile saline intratracheal injections. The mice in the control group were administered only sterile saline. The mice were then placed in a vertical position and rotated for 1 min to distribute the instillation in the lungs. Six hours later, the mice were sacrificed after being anesthetized.

Bronchoalveolar Lavage Fluid, Total Cell Counts, White Blood Cell Counts, and Protein Analysis

Six hours after LPS injection, the mice were exsanguinated under anesthesia. According to the previous report, BALF was collected at the upper part of the trachea using three rounds of lavage with 500 μL PBS (pH 7.2) each time. The fluid recovery rate was more than 90%. Lavage samples from the mice were kept on ice. The BALF was centrifuged at $700\times$ g for 5 min at $4\,^{\circ}C$ (Zhang *et al.*, 2010). The supernatant was removed and retained. The sedimented cells were resuspended in 2 mL PBS, of which 1 mL was used to detect total cell counts and WBC counts (Chen *et al.*, 2016) using a hemocytometer. The remaining cells were analyzed with a radioimmunoprecipitation assay buffer (RIPA buffer) and centrifuged to obtain the supernatant for detecting total protein content through a Bradford assay.

NO, TNF-α, IL-1ß and IL-6 in BALF

NO production was indirectly assessed by measuring the nitrite levels in the cultured media and BALF, determined using a colorimetric method based on the Griess reaction (Hu *et al.*, 2014). The BALF supernatant was collected after centrifugation (for 5 min at $700\times g$) and stored at $-80°C$ before the cytokine assay. TNF-α, IL-1β, and IL-6 in BALF were measured using an enzyme-linked immunosorbent assay kit obtained from ELISA R&D Systems (Minneapolis, MN, USA) by modifying a previously reported method (Yeh *et al.*, 2014). The detection limit of this method was greater than 7.8 pg/mL.

TNF-α and IL-6 in Lung, Liver, and Kidney Tissues

After being anesthetized, the mice were sacrificed to collect lung, liver, and kidney tissues to measure the inflammatory cytokines. In brief, lung, liver, and kidney tissue samples were placed in a homogenization buffer (0°C) at a ratio of 1 g/mL of PBS, then homogenized and centrifuged at $1000\times g$ at 4°C for 10 min (Li *et al.*, 2014). TNF-α and IL-6 in the lung, liver, and kidney were measured by an enzyme-linked immunosorbent assay kit from ELISA R&D Systems by modifying a previously reported method (Yeh *et al.*, 2014). The detection limit of this method was greater than 7.8 pg/mL.

Myeloperoxidase Activity Assay

After the BALF collection, the left upper lobe of the mice was removed, washed, and kept at $-80°C$. The steps were conducted according to the method of Bani *et al.* (1998) with some modifications. After weighing, the lungs were homogenized at $12,000\times g$ and 4°C for 15 min, and resuspended in 50 mM KPO_4 buffer (PH 6.0) containing 0.19 mg/mL of o-dianisidine chloride, and 0.0005% H_2O_2 was the substrate for myeloperoxidase (MPO) at 460 nm using a spectrophotometer (Molecular Devices, Sunnyvale, CA, USA). The results were expressed as units of MPO activity per gram of lung tissue.

Lung Wet to Dry Weight Ratio

The severity of the pulmonary edema was assessed by the wet to dry (W/D) ratio. The right lower lungs were weighed and then dehydrated at 60°C for 72 h in an oven (Zhou *et al.*, 2014).

Histopathological Analysis

At 6 h after treatment with LPS, mice were euthanized and samples of the middle lobe of the left lung were harvested and fixed in 4% paraformaldehyde in 0.1 M PBS (pH 7.4)

for 24 h at 4°C. For the light microscopic examination, the lung tissue was dehydrated with graded alcohol and then embedded in paraffin. Paraffin sections were stained with hematoxylin and eosin. Pathological changes in the lung tissues were observed under a light microscope (Parsey *et al.*, 1998). The score represented the severity of lung injury, which depended on the degree of inflammatory cell infiltration, WBC count, and diffuse alveolar damage. Based on the severity of lesions, a score was assigned on a scale of one to five. A score of 0 represented no abnormalities; 1 represented minimal (< 1%); 2 represented slight (1–25%); 3 represented moderate (26–50%); 4 represented moderate-to-severe (51–75%); and 5 represented severe-to-high (76–100%) (Chao *et al.*, 2017).

Western Blot Analysis of Lung Tissue

PBS and RIPA were added to the left lung tissue before grinding. The extract was then centrifuged at $12,000\times g$ for 15 min to obtain the supernatant. Bovine serum albumin (BSA) was used as a protein standard to calculate the equal total cellular protein amounts. Protein samples (50 μg) were resolved by denaturing 10% sodium dodecyl sulfate-polyacrylamide gel electrophoresis (SDS-PAGE) using standard methods, and then were transferred to PVDF membranes by electroblotting and blocking with 1% BSA. The membranes were probed with primary antibodies iNOS, COX-2, IκB, NF-κB, and phosphorylated and nonphosphorylated forms of MAPK p38, ERK, JNK, and proinflammatory enzymes (SOD, GPx, catalase) at 4°C overnight, washed three times with PBS with Tween 20, and incubated for 1 h at 37°C with horseradish-peroxidase-conjugated secondary antibodies. The membranes were washed three times before being inspected for immunoreactive proteins with enhanced chemiluminescence (ECL) using hyperfilm and ECL reagent. The results of the western blot analysis were quantified by comparing the relative intensity with that of the control by using Kodak Molecular Imaging Software.

Statistical Analysis

Unless otherwise stated, all experiments were performed at least three times independently. The data were presented as the mean ± standard deviation (SD) and statistical comparisons between the groups were performed using a one-way analysis of variance (ANOVA) followed by a Scheffe's multiple range test. A p-value of < 0.05 was considered significant.

Results

In Vitro Cytotoxicity

This experiment investigated whether asatone prevents cytotoxicity and NO production in RAW 264.7 cells challenged with LPS. Figure 1B indicates that the cell viability did

not appear to differ in all six groups. In other words, LPS in the presence of asatone (2.5–20 μg/mL) did not cause any significant cytotoxicity (less than 10%). Figure 1C demonstrates that asatone 2.5–20 μg/mL reduced NO production in a dose-dependent manner. As a result of these findings, asatone concentrations below or equal to 20 μg/mL were applied in all subsequent cellular and animal experiments.

Asatone Attenuates Pulmonary Inflammation and Edema in LPS-Induced ALI

To assess the lung histopathological changes in ALI, lung histological sections after hematoxylin and eosin (H&E) staining were evaluated. Figure 2A reveals that no lung injury was noted in the control group. Figure 2B shows a typical section from the LPS-induced group, revealing notable inflammatory neutrophil infiltration, interstitial edema, interalveolar septal thickening, and intra-alveolar and interstitial patchy hemorrhage. After pretreatments with DEX (Fig. 2C) and different concentrations of asatone (Figs. 2D–2F), these histopathological changes in lung tissues were alleviated. Figure 2G reveals that asatone pretreatment reduced histopathological changes in the lung tissues challenged with LPS.

The W/D ratio of lung weight is a critical feature of pulmonary edema in ALI/ARDS. Figure 3 reveals that the W/D ratio in the LPS-induced group was ameliorated by DEX (10 mg/kg) and asatone (10–40 mg/kg) in a dose-dependent manner. In other words, an LPS-induced pulmonary edema can be prevented with a pretreatment of DEX or asatone.

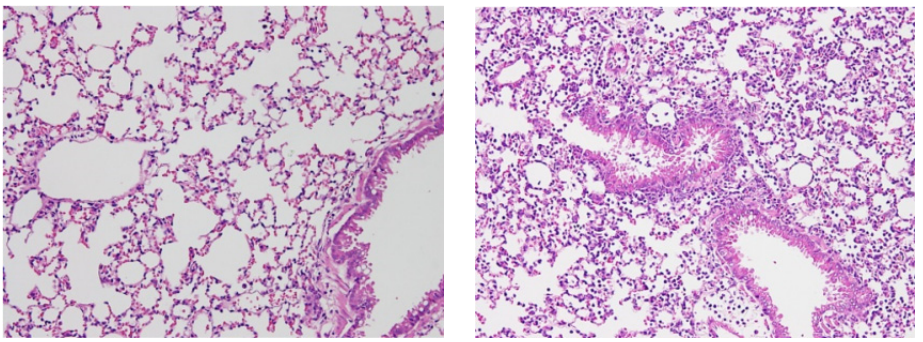

(A) (B)

Figure 2. Asatone attenuated *in vivo* pulmonary inflammation on histological sections. For this and the following experiments, acute pulmonary injury was induced by the injection of 5 mg/kg of LPS. One hour prior to LPS injection, the mice were pretreated with asatone as indicated. They were sacrificed under anesthesia at 6 h after the injection. Their left lungs were fixed with formalin to prepare the histological sections for staining with hematoxylin and eosin (H&E). The photographed section shows a representative view (×200) of each group. (A) Control; (B) LPS + Saline; (C) LPS + DEX (10 mg/kg); (D) LPS + Asatone-L (10 mg/kg); (E) LPS + Asatone-M (20 mg/kg); (F) LPS + Asatone-H (40 mg/kg); (G) Severity of lung injury was analyzed using the lung injury scoring system. Each value represents the mean ± SD of six mice. Statistical significance was analyzed using a one-way ANOVA followed by a Scheffe's multiple range test ($^{\#\#\#}p < 0.001$ compared with the control group. $^{*}p < 0.05$ and $^{**}p < 0.01$ compared with the LPS-induced group).

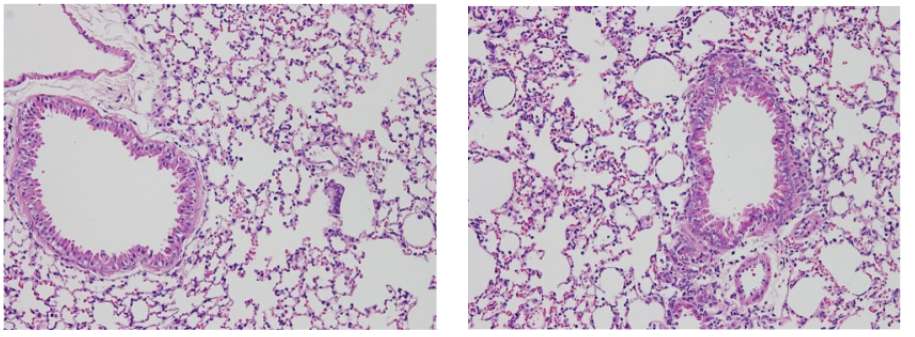

(C) (D)

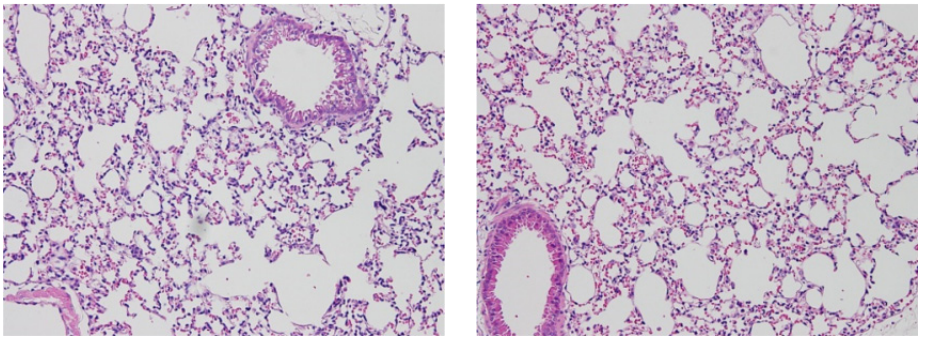

(E) (F)

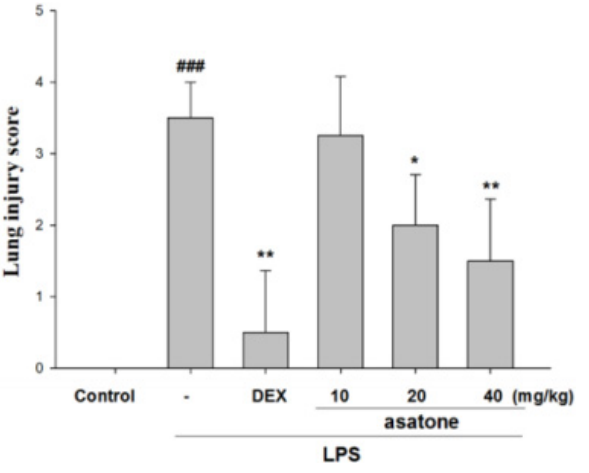

(G)

Figure 2. (*Continued*)

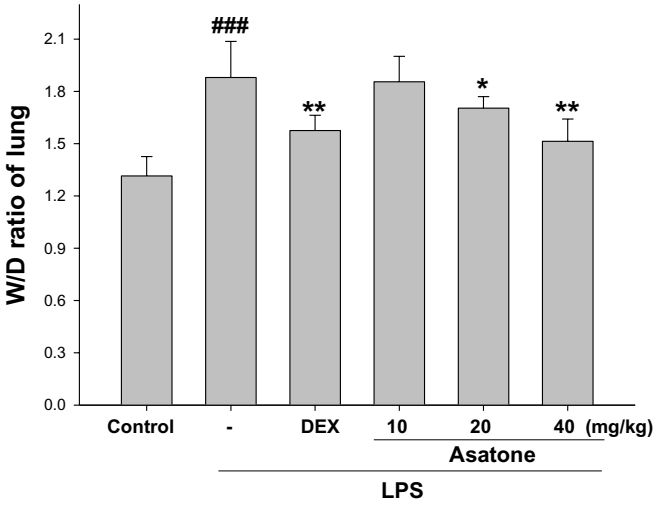

Figure 3. Asatone reduced *in vivo* pulmonary edema as evaluated by the wet to dry (W/D) ratio of the lung. As indicated in Fig. 2, mice were sacrificed under anesthesia and their right lungs were cut to assess the W/D ratio in six groups: control, LPS + saline (−), LPS + dexamethasone (DEX) 10 mg/kg, LPS + asatone 10 mg/kg, LPS + asatone 20 mg/kg, LPS + asatone 40 mg/kg. Each value represents the mean ± SD of six mice. $^{###}p < 0.001$ compared with the control group. $^{*}p < 0.05$ and $^{**}p < 0.01$ compared with the LPS group.

Asatone Reduces Total Cell Counts, Proteins, and WBC Counts in BALF in ALI

To further evaluate the anti-inflammatory property of asatone, the experiments measured the total cell counts and determined the total secreted proteins and WBC counts in the BALF (Figs. 4A–4C). The results demonstrated that LPS treatment increased the total cell counts (Fig. 4A), and the secreted proteins (Fig. 4B), and WBC counts (Fig. 4C) were markedly reduced by 10 mg/kg of DEX, and were reduced by 10–40 mg/kg of asatone in a dose-dependent manner.

Asatone Downregulates NO, TNF-α, IL-1ß, and IL-6 in BALF in ALI

NO and proinflammatory cytokines, TNF-α, IL-1β, and IL-6 in the BALF were further measured. Figures 5A–5D reveals that the concentrations of NO, TNF-α, IL-1β and IL-6 in BALF were markedly increased in mice treated with LPS. All these increases were most prominently inhibited by 10 mg/kg of DEX and 40 mg/kg of asatone. The inhibition of asatone at 10–40 mg/kg occurred in a dose-dependent manner.

Effects of Asatone on LPS-Induced TNF-α and IL-6 Production in Lung, Liver, and Kidney Tissues

As revealed in Figs. 5E and 5F, stimulation with LPS markedly increased the expression of TNF-α and IL-6 in the lung, liver, and kidney compared with the control group.

Pretreatment with asatone substantially attenuated LPS-induced TNF-α and IL-6 levels in lung and liver tissues, but not in kidney tissues (Figs. 5E and 5F).

Effects of Asatone on MPO and Antioxidative Enzyme Activities in BALF in ALI

Activated polymorphonucleocytes (PMNs) that produce MPO are linked to the production of oxidative stress. Figure 6A reveals that the level of MPO activity was clearly increased

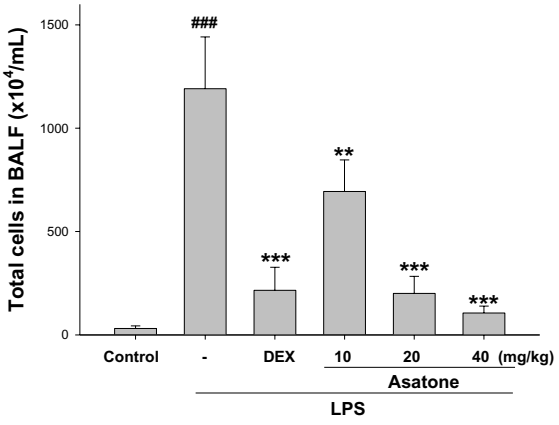

(A)

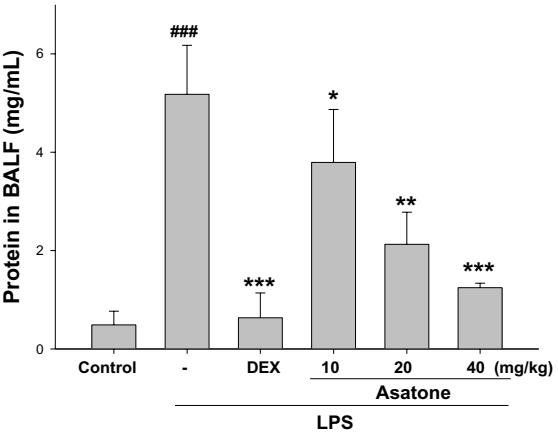

(B)

Figure 4. Asatone reduced total cell counts (A), total protein (B) and white blood cell counts (C) in bronchoalveolar lavage fluid (BALF). As indicated in Fig. 2, the mice were sacrificed under anesthesia and their lungs were lavaged. The BALF was collected to count the infiltrating leukocytes by hemocytometry, and to quantitate the total protein by a Bradford assay in six groups as described in Fig. 3. Each value represents the mean ± SD of six mice. $^{###}p < 0.001$ compared with the control group (one-way ANOVA followed by Scheffe's multiple range test). $^{*}p < 0.05$, $^{**}p < 0.01$, and $^{***}p < 0.001$ compared with the LPS group.

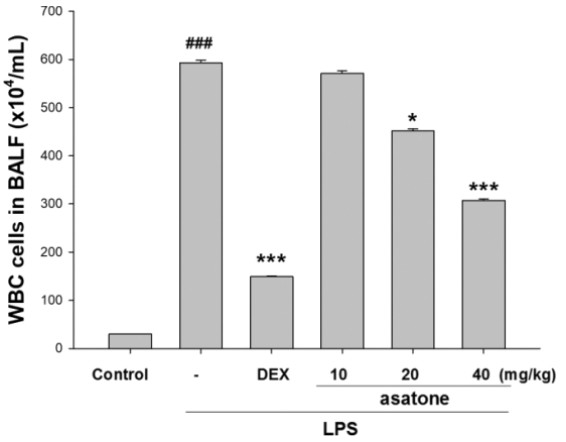

(C)

Figure 4. (*Continued*)

in the LPS-induced group ($p < 0.001$ vs. the control group). Pretreatments with 10 mg/kg of DEX and 40 mg/kg of asatone maximally inhibited the increased MPO activity, whereas 10–40 mg/kg of asatone dose-dependently inhibited this activity.

Antioxidative enzymes (AOEs) can ameliorate inflammatory activities in LPS-induced ALI in mice (Camacho-Barquero *et al.*, 2007; Hosakote *et al.*, 2009). Figure 6B reveals that expressions of AOEs including catalase, GPx, and SOD were all markedly reduced in the LPS-induced group ($p < 0.001$ vs. the normal control group). These reduced expressions were generally reversed by pretreatments with 40 mg/kg of asatone and 10 mg/kg of DEX. Asatone in particular demonstrated a superior effect on GPx expression.

Asatone Inhibits iNOS and COX-2 Proteins in Lung Tissue in ALI

We assessed the role of asatone in modulating LPS-induced cytokine proteins, iNOS, and COX-2. Using western blot analysis, we determined the levels of cytokine proteins in the lung tissue of the ALI mice. As presented in Fig. 7, the levels of iNOS and COX-2 proteins were significantly decreased in the asatone with LPS group compared with the LPS-induced group ($p < 0.001$).

Effects of Asatone on MAPK, IκB and NF-κB Activations in ALI Lung Tissue

We investigated whether asatone might affect the MAPK pathways (ERK, JNK, and p38) that stimulate the phosphorylation of NF-κB in ALI. Figure 8A

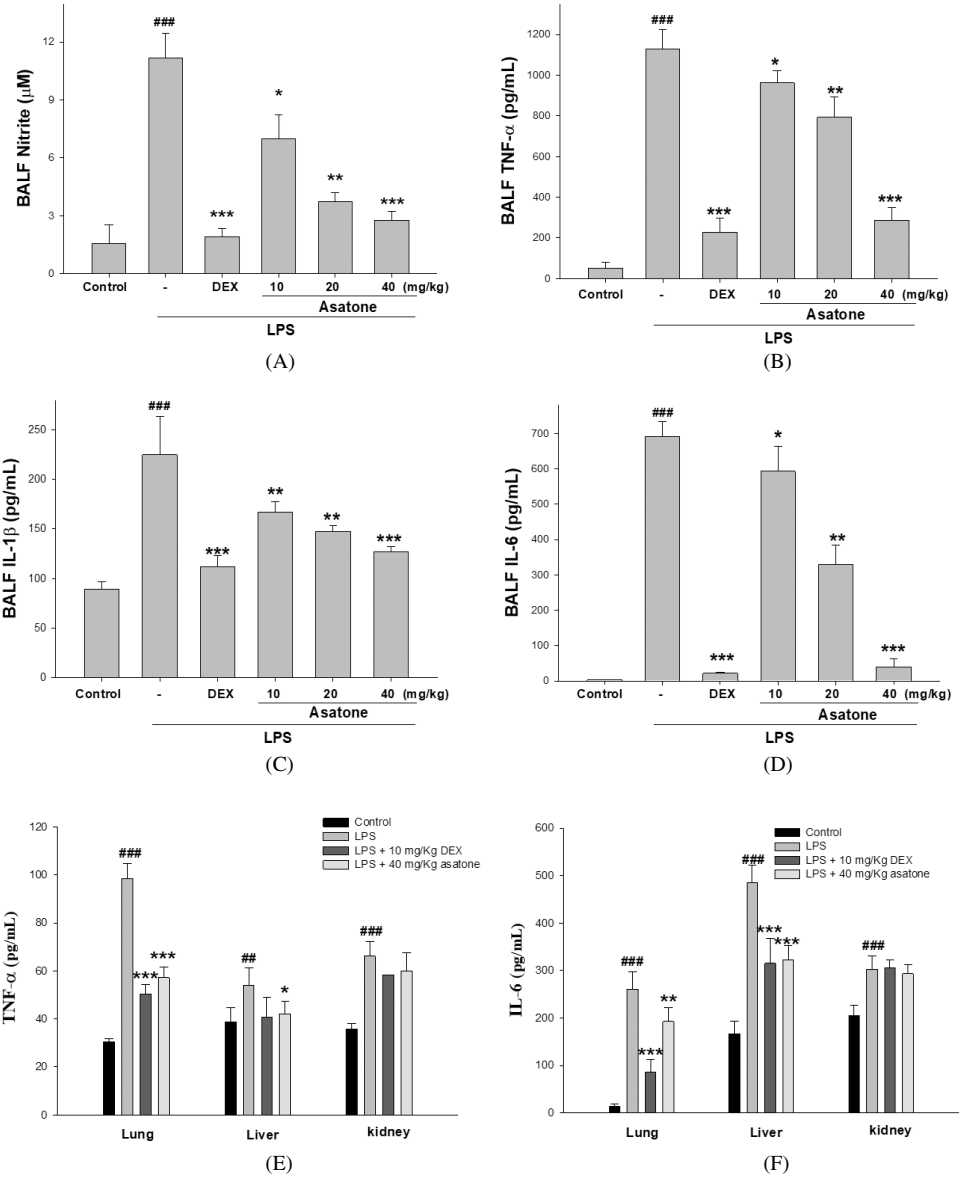

Figure 5. Asatone down regulated the level of NO (A),TNF-α (B), IL-1β (C) and IL-6 (D) in BALF of lung tissues and the level of TNF-α (E) and IL-6 (F) in the lung, liver, but not the level of kidney tissue. The BALF of lung was collected for quantitating NO, TNF-α, IL-1β, IL-6, and the tissues of lung, liver, and kidney were collected for quantitating TNF-α, and IL-6 by Bradford assay. Each value represents the mean ± SD of six mice. $^{\#\#}p < 0.01$ and $^{\#\#\#}p < 0.001$ compared with control group (One-way ANOVA followed by Scheffe's multiple range tests). $^{*}p < 0.05$, $^{**}p < 0.01$ and $^{***}p < 0.001$ were compared with LPS group.

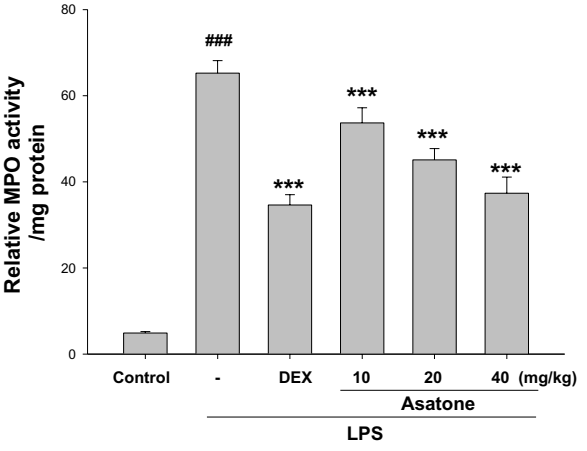

(A)

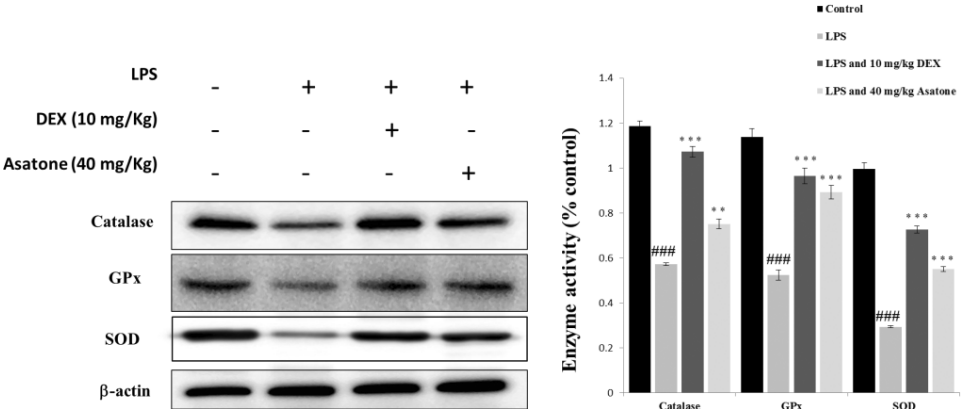

(B)

Figure 6. Asatone reduced the activation of (A) myeloperoxidase (MPO) activity and (B) antioxidative enzymes (SOD, GPx, and catalase) in the BALF. As indicated in Fig. 2, the mice were sacrificed under anesthesia and their lungs were lavaged. The BALF was collected to detect (A) MPO activity by ELISA reader in six groups as in Fig. 3. Detection of (B) catalase, GPx, SOD, and by Western blotting, however, was performed in four groups: control, LPS, LPS + DEX 10 mg/kg, and LPS + Asatone 40 mg/kg. Western blotting was performed using a specific antibody for the detections. The lower figure indicates a representative result of the western blotting. Data is represented as the mean ± SD of six mice. $^{###}p < 0.001$ compared with the control group sample (one-way ANOVA followed by Scheffe's multiple range tests). $^{**}p < 0.01$, and $^{***}p < 0.001$ compared with the LPS group.

reveals that LPS stimulation markedly increased the expressions of phosphorylated ERK, JNK, and p38, whereas 40 mg/kg of asatone and 10 mg/kg of DEX significantly inhibited these increased expressions. Conversely, Fig. 8B demonstrates that LPS stimulation markedly inhibited the expressions of NF-κB and IκBα, whereas

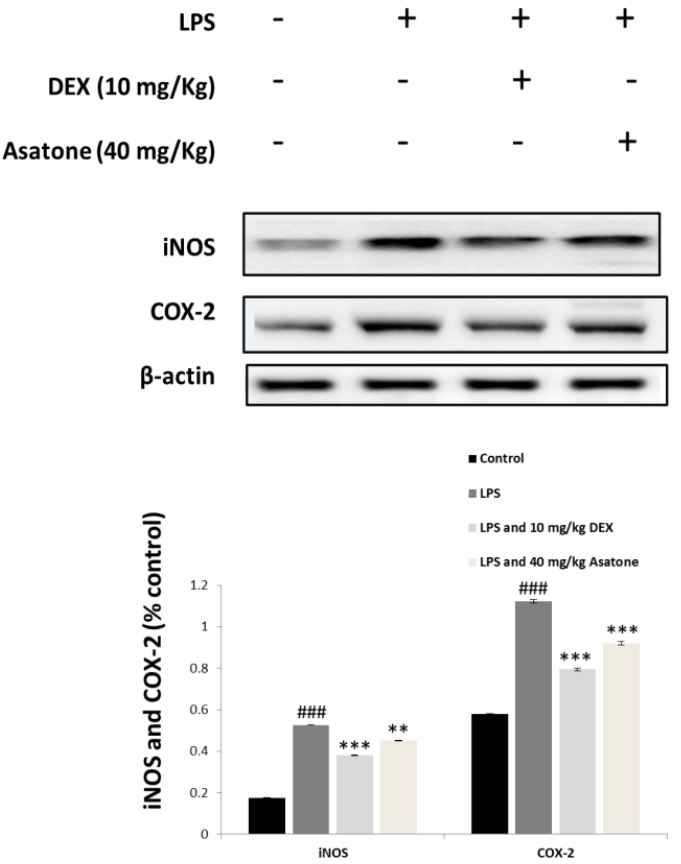

Figure 7. Asatone inhibited iNOS and COX-2 expression in the lung tissue. As indicated in Fig. 2, the mice were sacrificed under anesthesia. Their left lungs were cut and homogenized to extract protein. The protein was employed for the detection of iNOS and COX-2 expressions by Western blotting in four groups as described in Fig. 6B. A representative Western blot from two separate experiments is presented. The relative protein levels of iNOS and COX-2 in DEX- or asatone-pretreated lungs were calculated with reference to those of the LPS-stimulated culture. Data is represented as the mean ± SD of six mice. $^{###}p < 0.001$ compared with the control group. Each of the mice were evaluated in four groups as in Fig. 6B (one-way ANOVA followed by Scheffe's multiple range tests). $^{**}p < 0.01$ and $^{***}p < 0.001$ compared with the LPS group.

these inhibitions were effectively prevented by 40 mg/kg of asatone and 10 mg/kg of DEX.

MAPK pathways (ERK, JNK and p38) can stimulate the phosphorylation of NF-κB in LPS-induced ALI (Annapurna *et al.*, 2013), and NF-κB can prompt the transcription of proinflammatory cytokines including TNF-α, IL-1β, and IL-6, which is a crucial step in the pathogenesis of ALI (Bhaskaran *et al.*, 2010; Lin *et al.*, 2015). These data indicate that asatone inhibits LPS-induced NF-κB activation as well as p-MAPK pathways in the relief of LPS-induced ALI.

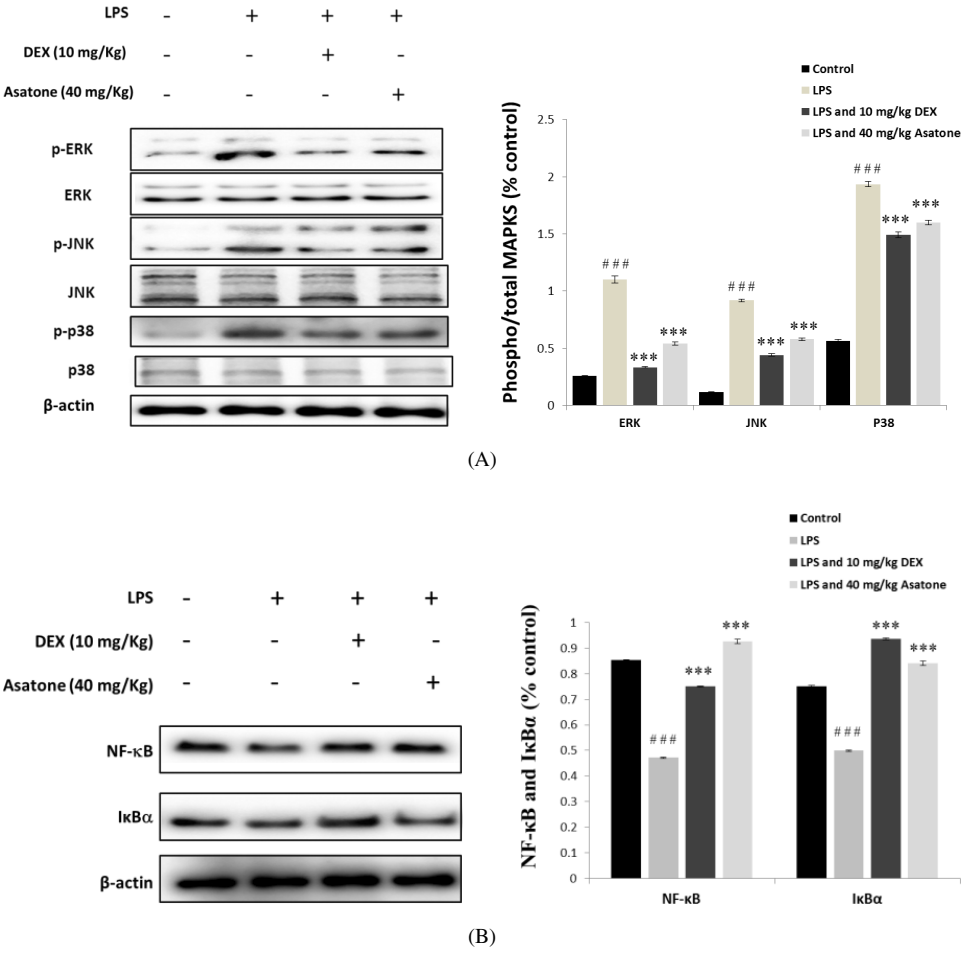

Figure 8. Effects of asatone on LPS-induced phosphorylation and nonphosphorylation protein expressions in ALI mice. As indicated in Fig. 2, the mice were sacrificed under anesthesia. Their left lungs were cut and homogenized to extract protein. The protein was used for the detection of (A) ERK, JNK, and p38, (B) NF-κB and IκBα in four groups as in Fig. 7. The fold change in protein expression between the treated and control groups was calculated. A representative western blot from two separate experiments is shown. Data is represented as mean ± SD of six mice. $^{###}p < 0.001$ compared with the sample of the control group (one-way ANOVA followed by Scheffe's multiple range tests). $^{***}p < 0.001$ compared with the LPS group.

Discussion

The *in vitro* studies revealed that LPS in the presence of asatone (2.5–20 μg/mL) led to nonsignificant cytotoxicity (Fig. 1B) and reduced NO production in a dose-dependent manner (Fig. 1C). The *in vivo* studies of ALI demonstrated that asatone reduced the histopathological changes in lung tissues (Fig. 2), pulmonary edema (W/D ratio) (Fig. 3), total cell counts, total proteins, and WBC counts in the BALF (Fig. 4). Furthermore,

asatone downregulated NO and proinflammatory cytokines, including TNF-α, IL-1β, and IL-6 in the BALF (Figs. 5A–5D). Stimulation with LPS markedly increased the expression of TNF-α and IL-6 in the lung, liver, and kidney compared with the control group; and pretreatment with asatone significantly attenuated LPS-induced TNF-α and IL-6 levels in lung and liver tissues, but not in kidney tissues (Figs. 5E and 5F). MPO activity in the BALF (Fig. 6A), iNOS and COX-2 cytokine protein expressions (Fig. 7), and the MAPK pathway in the lung tissue (Fig. 8A) were altered after asatone and DEX pretreatments. Furthermore, asatone increased AOEs in the BALF (Fig. 6B) and IκBα and NF-κB activations in the lung tissues (Fig. 8B). Taken together, asatone exerted anti-inflammatory effects by suppressing WBC infiltration in the lung and inhibiting the expression of key proinflammatory cytokines, probably through two different routes of IκBα, NF-κB, and p-MAPK.

A critical initial role in the pathogenesis of ALI/ARDS is the activation and recruitment of neutrophils that lead to pulmonary edema, the release of neutrophil elastase, myeloperoxidase (MPO), and proinflammatory cytokines (Li *et al.*, 2015a,b; Chen *et al.*, 2016), and two major anti-inflammatory pathways (Liu *et al.*, 2014; Li *et al.*, 2015a; Chen *et al.*, 2016). This is consistent with our findings that LPS increased cell infiltrations in the lung tissue (Figure 2), pulmonary edema (Fig. 3), total cell counts, total proteins, and WBC counts (Fig. 4), NO and proinflammatory cytokines including TNF-α, IL-1β, and IL-6 in the BALF (Figs. 5A–5D), and affected LPS-induced TNF-α and IL-6 production in the lung and liver, but not in the kidney (Figs. 5E and 5F) (Li *et al.*, 2014). MPO activity in the BALF (Fig. 6A) and iNOS and COX-2 protein expressions (Fig. 7) were increased, but AOEs (Figure 6B) and NF-κB and IκB expressions in the lung tissues (Fig. 8B) were decreased. Although the increased cellular infiltration directly caused by LPS (Figs. 2 and 4) plays a crucial initial role in the pathogenesis of ALI/ARDS, it may also be reciprocally caused by LPS-induced changes, as revealed in Figs. 4–8. Nevertheless, asatone pretreatments reversed these LPS-induced changes. The reversions in LPS-induced cellular infiltration (Figs. 2 and 4) may also have been reciprocally caused by the asatone-reversed changes (Figs. 4–8).

ALI/ARDS are defined by a series of histologic changes, such as pulmonary edema, neutrophil infiltration, and cellular protein secretion (Tunceroglu *et al.*, 2013; Huang *et al.*, 2014a). Consistent with these concepts, we demonstrated that LPS increased cell infiltrations in the lung tissue (Fig. 2), total proteins (Fig. 4B), and WBC counts (Fig. 4C). Asatone reduced the activation and recruitment of WBC (Fig. 4C). This study demonstrated that LPS challenge led to an increase in total cell counts, total proteins, and WBC counts in BALF, and these increases were attenuated by asatone pretreatment (Fig. 4). Therefore, we concluded that asatone can reduce total cell counts, total proteins, and WBC counts, but we could not ascertain whether this effect may also result in other forms of improvement, as revealed in Figs. 3–8.

The transcription factor NF-κB is critical for controlling multiple key cellular processes (Huang *et al.*, 2014a). Through the inhibition of the NF-κB pathway, the subsequent inhibition of the expression of proinflammatory cytokines (TNF-α, IL-1β, and IL-6) led to a recovery from septic dysfunction (Huang *et al.*, 2014a). These conclusions were supported

by the results of our present study. LPS stimulation increased the production of proinflammatory cytokines, and this increased production was reduced by asatone pretreatment in the BALF (Figs. 5A–5D). The results demonstrated that asatone markedly reduced the levels of TNF-α and IL-6 in the lung and liver, but not in the kidney (Figs. 5E and 5F) (Li *et al.*, 2014). Another experiment revealed that asatone pretreatment inhibited the degradation of NF-κB in the LPS-induced ALI in the lungs (Fig. 8B). Therefore, the results also indicated that asatone reduced leukocyte infiltration in the lungs by decreasing the expression of proinflammatory cytokines.

NO and prostaglandins are produced by the activation of iNOS and COX-2, respectively. They are proinflammatory molecules that play important roles in inflammatory responses (Zamora *et al.*, 2000; Giuliano and Warner, 2002). Our results indicated that LPS prominently activated both iNOS and COX-2 proteins, whereas asatone inhibited them (Fig. 7). Although we did not determine prostaglandin levels, the LPS-induced NO production was concentration-dependently inhibited by asatone in RAW264.7 cells (Fig. 1C). Therefore, iNOS and COX-2 protein production inhibition should be considered as strategies for the treatment of related inflammatory diseases. Our results also suggest that IL-1β, IL-6, and TNF-α were direct targets of asatone, and asatone suppressed downstream signaling pathways to decrease iNOS and COX-2 protein expressions (Fig. 7).

Activated polymorphonucleocytes (PMNs) that produce myeloperoxidase (MPO) have been linked to the production of oxidative stress. AOEs (catalase, SOD, and GPx) are activated when cells respond to inflammation and oxidative stress and have crucial functions in maintaining redox homeostasis in cells (Shie *et al.*, 2015). LPS-induced mouse ALI is characterized by prominent neutrophil infiltration that reduces AOE activity in lung tissues (Yang *et al.*, 2012). The present study demonstrated that asatone pretreatment potently inhibited WBC infiltration (Figs. 2 and 4), lung edema (Fig. 3), proinflammatory cytokines (Fig. 5), and MPO activity (Fig. 6A). Conversely, asatone increased the intracellular AOEs (Fig. 6B). Whether these increased intracellular AOEs were directly promoted by asatone or this increase indirectly resulted from the improved conditions exerted by asatone (Figures 2–6) was beyond the scope of this study.

Activated PMNs that produce MPO are linked to the production of oxidative stress and inflammatory stimuli by LPS, which leads to the activation of MAPK and NF-κB (Penga *et al.*, 2016). Inhibiting NF-κB and MAPK pathways have been suggested as the two major mechanisms underlying the attenuation of LPS-induced inflammatory cytokine production. NF-κB is the transcription factor in regulating many proinflammatory cytokine genes. MAPKs play a critical role in the control of cellular responses to cytokines and stressors (Huang *et al.*, 2014b). Moreover, MAPKs are involved in the LPS-induced signaling pathway by which iNOS is expressed. In the present study, we demonstrated that NF-κB (Fig. 8B) and the phosphorylation of MAPKs can be induced by LPS (Fig. 8A). Asatone pretreatment significantly inhibited LPS-induced ERK, JNK, and p38 phosphorylation.

This study is the first to reveal the anti-inflammatory effect of asatone in LPS-stimulated ALI and relate this effect with various molecular mechanisms: transcription factors (iNOS, COX-2, MPO, AOEs, IκB, NF-κB, and MAPK) and proinflammatory cytokines (TNF-α,

IL-1β and IL-6). These data indicate that asatone is a potential novel therapeutic drug for treating inflammatory diseases in various organs.

Acknowledgments

The authors thank the financial supports from the National Science Council (MOST 105-2320-B-039-046 and MOST 106-2320-B-039-045), China Medical University (CMU) (ASIA104-CMUH-06 and CMU105-ASIA-23), Asis University (105-ASIA-05, 105-ASIA-06 and 105-ASIA-07) and Tzu Chi University (TCCCF-P-103003) for financial support. This manuscript was read by Professor J. S. Kuo and edited by Wallace Academic Editing.

References

Annapurna, A., M.A. Ansari and P.M. Manjunath, Partial role of multiple pathways in infarct size limiting effect of quercetin and rutin against cerebral ischemia-reperfusion injury in rats. *Eur. Rev. Med. Pharmacol. Sci.* 17: 491–500, 2013.

Bani, D., E. Masini, M.G. Bello, M. Bigazzi and T.B. Sacchi. Relaxin protects against myocardial injury caused by ischemia and reperfusion in rat heart. *Am. J. Pathol.* 152: 1367–1376, 1998.

Bhaskaran, N., S. Shukla, J.K. Srivastava and S. Gupta. Chamomile: An anti-inflammatory agent inhibits inducible nitric oxide synthase expression by blocking RelA/p65 activity. *Int. J. Mol. Med.* 26: 935–940, 2010.

Bhaskaran, N., J.K. Srivastava, S. Shukla and S. Gupta. Chamomile confers protection against hydrogen peroxide-induced toxicity through activation of Nrf2-mediated defense response. *Phytother. Res.* 27: 118–125, 2013.

Camacho-Barquero, L., I. Villegas, J.M. Sanchez-Calvo, E. Talero, S. Sanchez-Fidalgo, V. Motilva and C. Alarcon de la Lastra. Curcumin, a *Curcuma longa* constituent, acts on MAPK p38 pathway modulating COX-2 and iNOS expression in chronic experimental colitis. *Int. Immunopharmacol.* 7: 333–342. 2007.

Chao, W., J.S. Deng, S.S. Huang, P.Y. Li, Y.C. Liang and G.J. Huang. 3,4-Dihydroxybenzalacetone attenuates lipopolysaccharide-induced inflammation in acute lung injury via down-regulation of MMP-2 and MMP-9 activities through suppressing ROS-mediated MAPK and PI3K/AKT signaling pathways. *Int. Immunopharmacol.* 50: 77–86. 2017.

Chen, H., C. Bai and X. Wang. The value of the lipopolysaccharide-induced acute lung injury model in respiratory medicine, *Expert Rev. Respir. Med.* 4: 773–783, 2010.

Chen, J.J., C.C. Huang, H.Y. Chang, P.Y Li, Y.C. Liang, J.S. Deng, S.S. Huang and G.J. Huang. Scutellaria baicalensis ameliorates acute lung injury by suppressing inflammation *in vitro* and in vivo. *Am. J. Chin. Med.* 45: 1–21, 2016.

Chien, T.M., P.C. Hsieh, S.S. Huang, J.S. Deng, Y.L. Ho, Y.S. Chang and G.J. Huang. Acanthopanax trifoliatus inhibits lipopolysaccharide-induced inflammatory response *in vitro* and in vivo. *Kaohsiung J. Med. Sci.* 31: 499–509, 2015.

Dan, Y., H.Y. Liu, W.W. Gao and S.L. Chen. Activities of essential oils from asarum heterotropoies var. mandshurium against five phytopathogens. *Crop Prot.* 29: 295–299, 2010.

Drew, A.K., I.M. Whyte, A. Bensoussan, A.H. Dawson, X. Zhu and S.P. Myers. Chinese herbal medicine toxicology database: Monograph on herba asari, "Xi_Xin". *J. Toxicol. Clin. Toxicol.* 40: 169–172, 2002.

Giuliano, F. and T.D. Warner. Origins of prostaglandin E2: Involvements of cyclooxygenase (COX)-1 and COX-2 in human and rat systems. *J. Pharmacol. Exp. Ther.* 303: 1001–1006, 2002.

Hayashi, N., Y. Yamamura, S. Ôhama and H. Komae. Asatone in *Asarum* (Aristolochiaceae). *Phytochemistry* 15: 1567–1568, 1976.

Hosakote, Y.M., T. Liu, S.M. Castro, R.P. Garofalo and A. Casola. Respiratory syncytial virus induces oxidative stress by modulating antioxidant enzymes. *Am. J. Respir. Cell Mol. Biol.* 41: 348–357, 2009.

Hu, B., H. Zhang, X. Meng, F. Wang and P. Wang. Aloe-emodin from rhubarb (*Rheum rhabarbarum*) inhibits lipopolysaccharide-induced inflammatory responses in RAW264.7 macrophages. *J. Ethnopharmacol.* 153: 846–853, 2014.

Huang, K.L., C.S. Chen, C.W. Hsu, M.H. Li, H. Chang, S.H. Tsai and S.J. Chu. Therapeutic effects of baicalin on lipopolysaccharide-induced acute lung injury in rats. *Am. J. Chin. Med.* 36: 301–311, 2008.

Huang, G.J., J.S. Deng, C.C. Chen, C.J. Huang, P.J. Sung, S.S. Huang and Y.H. Kuo. Methanol extract of antrodia camphorata protects against lipopolysaccharide-induced acute lung injury by suppressing NF-κB and MAPK pathways in mice. *J. Agric Food Chem.* 62: 5321–5329, 2014a.

Huang, S.S., J.S. Deng, J.G. Lin, C.Y. Lee and G.J. Huang. Anti-inflammatory effects of trilinolein from panax notoginseng through the suppression of NF-κB and MAPK expression and proinflammatory cytokine expression. *Am. J. Chin. Med.* 42: 1485–1506, 2014b.

Khan, S., R.J. Choi, O. Shehzad, H.P. Kim, M.N. Islam, J.S. Choi and Y.S. Kim. Molecular mechanism of capillarisin-mediated inhibition of MyD88/TIRAP inflammatory signaling in *in vitro* and *in vivo* experimental models. *J. Ethnopharmacol.* 145(2): 626–637, 2013.

Kim, S.J., C.G. Zhang and J.T. Lim. Mechanism of anti-nociceptive effects of asarum sieboldii Miq. radix: Potential role of bradykinin, histamine and opioid receptor-mediated pathways. *J. Ethnopharmacol.* 88: 5–9, 2003.

Kosuge, T., M. Yokota, H. Nukaya, Y. Gotoh and M. Nagasawa. Studies on antitussive principles of Asiasari radix. *Chem. Pharm. Bull.* 26(7): 2284–2285, 1978.

Lee, J.Y., S.S. Moon and B.K. Hwang. Isolation and antifungal activity of kakuol, a propiophenone derivative from Asarum sieboldii rhizome. *Pest. Manag. Sci.* 61: 821–825, 2005.

Li, K.C., Y.L. Ho, W.T. Hsieh, S.S. Huang, Y.S. Chang and G.J. Huang. Apigenin-7-glycoside prevents LPS-induced acute lung injury via downregulation of oxidative enzyme expression and protein activation through inhibition of MAPK phosphorylation. *Int. J. Mol. Sci.* 16: 1736–1754, 2015a.

Li, K.C., Y.L. Ho, G.J. Huang and Y.S. Chang. Anti-oxidative and Anti-inflammatory effects of *Lobelia Chinensis in vitro* and *in vivo*. *Am. J. Chin. Med.* 43(2): 269–287, 2015b.

Li, P., Q.L. Liang, X.D. Cui, J. Li, N.S. Zou, Q.N. Wu and J.A. Duan. Protective effects of the active fraction from the tuber of *Scirpus Yagara* in mouse endotoxin shock model. *J. Ethnopharmacol.* 158: 331–337, 2014.

Lin, M.H., M.C. Chen, T.H. Chen, H.Y. Chang and T.C. Chou. Magnolol ameliorates lipopolysaccharide-induced acute lung injury in rats through PPAR-γ-dependent inhibition of NF-kB activation. *Int. Immunopharmacol.* 28: 270–278, 2015.

Liu, S.H., T.H. Lu, C.C. Su, I.S. Lay, H.Y. Lin, K.M. Fang, T.J. Ho, K.L. Chen, Y.C. Su, W.C. Chiang and Y.W. Chen. Lotus leaf (*Nelumbo Nucifera*) and its active constituents prevent inflammatory responses in macrophages via JNK/NF-κB signaling pathway. *Am. J. Chin. Med.* 42: 869–889, 2014.

Liu, Y., H. Wu, Y. C. Nie, J. L. Chen, W. W. Su and P. B. Li. Naringin attenuates acute lung injury in LPS-treated mice by inhibiting NF-κB pathway. *Int. Immunopharmacol.* 11: 1606–1612, 2011.

Parsey, M.V., R.M. Tuder and E. Abraham. Neutrophils are major contributors to intraparenchymal lung IL-1 beta expression after hemorrhage and endotoxemia. *J. Immunol.* 160: 1007–1013, 1998.

Penga, S., N. Hang, W. Liu, W. Guo, C. Jiangb, X. Yang, Q. Xua and Y. Sun. Andrographolide sulfonate ameliorates lipopolysaccharide-induced acute lung injury in mice by down-regulating MAPK and NF-κB pathways. *Acta Pharm. Sin. B* 6: 205–211, 2016.

Shie, P.H., S.S. Huang, J.S. Deng and G.J. Huang. Spiranthes sinensis suppresses production of pro-In*f*lammatory mediators by down-regulating the NF-kB signaling pathway and up-regulating HO-1/Nrf2 anti-oxidant protein. *Am. J. Chin. Med.* 43: 969–989, 2015.

Su, C.F., S.J. Kao and H.I. Chen. Acute respiratory distress syndrome and lung injury: Pathogenetic mechanism and therapeutic implication. *World J. Crit. Care Med.* 1: 50–60, 2012.

Tsai, C.L., Y.C. Lin, H.M. Wang and T.C. Chou. Baicalein, an active component of *Scutellaria baicalensis*, protects against lipopolysaccharide-induced acute lung injury in rats. *J. Ethnopharmacol.* 153: 197–206, 2014.

Tunceroglu, H., A. Shah, J. Porhomayon and N. D. Nader. Biomarkers of lung injury in critical care medicine: Past, present, and future. *Immunol. Invest.* 42: 247–261, 2013.

Wang, Z.J., B. Tabakoff, S.R. Levinson and T. Heinbockel. Inhibition of Nav1.7 channels by methyl eugenol as a mechanism underlying its antinociceptive and anesthetic actions. *Acta Pharmacol. Sin.* 36: 791–799, 2015.

Yamamura, S., Y.P. Chen, H.Y. Hsu and Y. Hirata. Asatone in plants of the aristolochiaceae. *Phytochemistry* 15: 426–427, 1976.

Yang, R., L. Yang, X. Shen, W. Cheng, B. Zhao, K. H. Ali, Z. Qian and H. Ji. Suppression of NF-κB pathway by crocetin contributes to attenuation of lipopolysaccharide-induced acute lung injury in mice. *Eur. J. Pharmacol.* 674: 391–396, 2012.

Yeh, C.H., J.J. Yang, M.L. Yang, Y.C. Li and Y.H. Kuan. Rutin decreases lipopolysaccharide-induced acute lung injury via inhibition of oxidative stress and the MAPK-NF-κB pathway. *Free Radic. Biol. Med.* 69: 249–257, 2014.

Zamora, R., Y. Vodovotz and T.R. Billiar. Inducible nitric oxide synthase and inflammatorydiseases, *Mol. Med.* 6: 347–373, 2000.

Zhang, X., H. Huang, T. Yang, Y. Ye, J. Shan, Z. Yin and L. Luo. Chlorogenic acid protects mice against lipopolysaccharide-induced acute lung injury. *Injury* 41: 746–752, 2010.

Zhou, E., Y. Li, Z. Wei, Y. Fu, H. Lei, N. Zhang, Z. Yang and G. Xie. Schisantherin a protects lipopolysaccharide-induced acute respiratory distress syndrome in mice through inhibiting NF-κB and MAPKs signaling pathways. *Int. Immunopharmacol.* 22: 133–140, 2014.